

1-1-2005

# Comparative three-dimensional imaging of living neurons with confocal and atomic force microscopy

Helen McNally

*Purdue University*, [mcnallyh@purdue.edu](mailto:mcnallyh@purdue.edu)

Bartek Rajwa

[brajwa@purdue.edu](mailto:brajwa@purdue.edu)

Jennifer Sturgis

*Purdue University*, [jesturgis@purdue.edu](mailto:jesturgis@purdue.edu)

J. Paul Robinson

*Purdue University*, [joseph.p.robinson.1@purdue.edu](mailto:joseph.p.robinson.1@purdue.edu)

Follow this and additional works at: <http://docs.lib.purdue.edu/nanodocs>

---

McNally, Helen; Rajwa, Bartek; Sturgis, Jennifer; and Robinson, J. Paul, "Comparative three-dimensional imaging of living neurons with confocal and atomic force microscopy" (2005). *Other Nanotechnology Publications*. Paper 59.  
<http://docs.lib.purdue.edu/nanodocs/59>

This document has been made available through Purdue e-Pubs, a service of the Purdue University Libraries. Please contact [epubs@purdue.edu](mailto:epubs@purdue.edu) for additional information.

# Comparative three-dimensional imaging of living neurons with confocal and atomic force microscopy

Helen A. McNally<sup>a,\*</sup>, Bartek Rajwa<sup>b,c</sup>, Jennie Sturgis<sup>b</sup>, J. Paul Robinson<sup>b,c</sup>

<sup>a</sup> Center for Paralysis Research, School of Veterinary Medicine, Purdue University, West Lafayette, IN 47906-2065, USA

<sup>b</sup> Cytometry Laboratories, School of Veterinary Medicine, Purdue University, West Lafayette, IN 47907-2064, USA

<sup>c</sup> Department of Biomedical Engineering, School of Engineering, Purdue University, West Lafayette, IN 47906-2016, USA

Received 12 April 2004; received in revised form 11 August 2004; accepted 13 August 2004

## Abstract

Atomic force microscopy applications extend across a number of fields; however, limitations have reduced its effectiveness in live cell analysis. This report discusses the use of AFM to evaluate the three-dimensional (3-D) architecture of living chick dorsal root ganglia and sympathetic ganglia. These data sets were compared to similar images acquired with confocal laser scanning microscopy of identical cells. For this comparison we made use of visualization techniques which were applicable to both sets of data and identified several issues when coupling these technologies. These direct comparisons offer quantitative validation and confirmation of the character of novel images acquired by AFM. This paper is one in a series emphasizing various new applications of AFM in neurobiology.

© 2004 Elsevier B.V. All rights reserved.

**Keywords:** Atomic force microscopy; Confocal laser scanning microscopy; Neurogenesis; Neurotrauma; Neurobiology

## 1. Introduction

The utilization of atomic force microscopy (AFM) to image living biological materials in their native environment with molecular or submolecular resolution is developing with great interest to the biological and medical communities (Morris et al., 2001). In the area of neuroscience, the application of AFM to neurons has been limited (Ricci et al., 2004) and has concentrated on internal organelles (Parpura et al., 1993; Lal et al., 1995) or nanoscale features of the surface, including gap junctions, ionic channels, and focal adhesion points (Jena, 1997). Others have used AFM technology to image neurons in the fixed state (Tojima et al., 2000; Weissmuller et al., 2000; Melling et al., 2001). However, the overall architecture of living neurons at high resolution has not been thoroughly evaluated with this technology until the first report in this series (McNally and Borgens, 2004). In this work we have utilized AFM and confocal laser scanning

microscopy (CLSM) to evaluate and confirm novel 3-D architectures of chick dorsal root ganglia (DRG) and sympathetic neurons. Such previously unreported architectures include transitory spines, ridges, and extensions of the soma and growth cone—particularly in the vertical plane. These preliminary data were confirmed with confocal imaging of similar neurons and comparison of the AFM data by confocal image processing techniques.

In contrast to AFM, confocal technology has been used for many years by the biological community to map biological pathways and understand intracellular mechanisms, as well as to view the overall architectures of living cells (Pawley, 1995; Matsumoto, 2002). For example, CLSM has been employed for the study of neural development (Niell and Smith, 2004), and of damage and repair of neural cells (Gallant and Galbraith, 1997; Hennig and Cotanche, 1998; Sah and Schwartz-Bloom, 1999). This can be accomplished with fast scan rates and very high magnification of living biological materials. However, the resolution of far-field optical systems like CLSM is limited by the wavelength used and by the numerical aperture (NA) of the objective. This

\* Corresponding author. Tel.: +1 765 494 4338; fax: +1 765 494 7605.  
E-mail address: mcnallyh@purdue.edu (H.A. McNally).

relationship indicates that when a high-NA lens and 500 nm wavelength are used, the smallest resolvable distance is approximately 200 nm (Piston, 1998). For the same conditions the axial resolution varies between 400 and 1900 nm depending on the size of the confocal aperture. Generally speaking, in a confocal instrument the  $z$ -resolution is reduced by about two-fold relative to the lateral resolution. Resolution using AFM is typically 1 nm in the  $x/y$  plane and 0.1 nm in the  $z$ -axis (Binnig and Quate, 1986). The increased resolution in the  $z$ -axis is of particular importance to these images of neural somas and growth cones with rapidly appearing and disappearing cytoplasmic projections in this axis.

Previous combinations of AFM and confocal instruments have been reported for biological applications (Henderson and Sakaguchi, 1993; Schabert et al., 1994; Vesenka et al., 1995). In this report we have utilized stand-alone AFM and confocal systems separately but imaged cells under similar conditions. To confirm the AFM analysis of living neurons, we combined and compared these two imaging modalities using a common format.

To introduce the use of AFM technology for neuroscience applications we have limited this report to the study of the 3-D architectures of living neurons. However, the versatility of AFM can be harnessed for many novel experiments in neurobiology. For example, we have recently used the AFM tip to produce nanoscale injury to the plasmalemma of growth cones and somas of DRG cells, subsequently imaging the responses of the cell to this damage with the same instrument (McNally and Borgens, 2004). AFM allows mechanical interaction with the sample, suggesting future studies into the form and function of localized areas. Physical characteristics of the living neuron's membrane, organelles, and cytoskeleton may be quantitatively investigated with AFM, providing more understanding of neurogenesis and neurotrauma.

## 2. Materials and methods

### 2.1. Sample preparation

Dorsal root ganglia (DRG) and sympathetic ganglia were dissected from 7- to 8-day-old chick embryos by conventional methods (Mahanthappa and Patterson, 1998). Individual neurons were obtained from the tissue using titration, enzymatic digestion (trypsin in Puck's medium), and differential centrifugation. Cell suspensions were moved to 35 mm Petri dishes and cell density within these samples was monitored using a hemocytometer. For the purposes of this study we attempted to obtain primary cultures on the order of 40,000 cells/35 mm Petri dish (1 cell/100  $\mu\text{m}^2$ ). The cells were plated on a substrate of polyornithine and laminin, and maintained at 37 °C in 5% CO<sub>2</sub>. Healthy DRG neurons on laminin, for example, will attach to the substrate and begin to form processes within 24 h. A conventional 2% neuron growth medium (Higgins and Banker, 1998) containing nerve growth factor (NGF), vitamin C, insulin (Sigma Chem. Co.

# I-6634), and penicillin/streptomycin (Sigma Chem. Co. # P-0906) was used in these studies. The base medium was prepared from an F-12 nutrient mixture (Gibco # 21700–075), supplemented with the other adjuncts, including conalbumin (Sigma # C-0880) and horse serum (Gibco # 26050–088), to a final pH of  $\sim 7.4$ , and refrigerated until used.

Preparation of samples to be imaged with both AFM and confocal systems required specific sample configurations. The high-numerical aperture objective of the confocal system required a sample substrate of glass of 0.17 mm thickness. The polyornithin/laminin coating did not interfere with the optical imaging since its thickness did not surpass the objective working distance. A sample to be imaged with AFM must be extremely flat ( $\leq 50$  nm RMS.) The surface of a polyornithin/laminin coated glass slide is  $20 \pm 5$  nm. The culture dish which maintains the cells in 2% neural media during imaging must be of specific geometry to accommodate the AFM and its associated fluid cell. The AFM support structure and fluid cell must not contact the culture dish sides during scanning or the area to be imaged will be lost and the tip damaged. In our system, this requires an area no less than 12.7 mm for the fluid cell but no greater than 40 mm to fit the AFM electronics. The depth of the dish must be sufficient to allow the AFM tip to contact the surface and be deep enough to avoid gas/fluid interface forces. A depth of 2–3 mm is sufficient. Finally, to coordinate experiments between AFM and confocal systems on identical cells, a method of identifying the location of interest for imaging was necessary. Our culture dish was a standard 35 mm Petri dish with a 13 mm area drilled from the bottom of the dish. A cover slip with etched grid (Electron Microscopy Sciences, #72264–23) was attached using Sylgard. The polyornithine and laminin coatings were applied. The cells were plated at the desired concentration and allowed to develop for 1–2 days.

### 2.2. Confocal imaging

In order to visualize morphology of the cells, the fluorescent lipophilic tracer *N*-(3-triethylammoniumpropyl)-4-(4-(dibutylamino)styryl) pyridinium dibromide (Molecular Probes, OR) was used to stain the cultures. This water-soluble dye, known as FM 1-43, is nontoxic to cells and remains non-fluorescent in aqueous medium. It is believed to insert itself into the outer leaflet of the cell membrane, where it becomes intensely fluorescent (Ryan et al., 1997; Ryan, 2001).

Confocal laser scanning microscopy was performed with a Bio-Rad Radiance 2100 Rainbow instrument (Bio-Rad Laboratories, Hemel Hempstead, UK) based on an inverted Nikon Eclipse TE2000 microscope (Nikon, Japan). The confocal system was equipped with a 60 $\times$  PlanApo 1.4-NA oil-immersion objective lens, an air-cooled, 100 mW output argon laser, three fluorescence detection channels (photomultipliers), and a nonconfocal transmitted light detector. Blue laser light attenuated to 3.5% of the maximum power was introduced into the sample. One of the photomultipliers was used to collect fluorescence signals from the green and

yellow region of the fluorescence emission, and the nonconfocal transmitted light detector was used to collect bright-field images. Fluorescence signals from the FM 1-43 probe passed through a 560 nm dichroic long-pass filter, a 500 nm laser-blocking filter and a 570 nm long pass-filter before being detected by a photomultiplier.

### 2.3. AFM imaging

The culture dishes containing developing neurons were removed from incubation, at which time temperature, humidity, and CO<sub>2</sub> levels were no longer controlled. To minimize cell changes due to these effects, experiments never exceeded 4 h, at which time cells were still healthy and well attached to the substrate. Cultured cells were rinsed with warmed medium and covered with 2 ml of neural medium. The samples were examined under a Nikon inverted microscope with a 10× objective to choose viable cells at relatively low density when individual neurons and their processes would not be at confluence (inset in Fig. 1). Neural cells and growth cones were identified and rated based on the character of their attachment to the culture substrate. For samples to be imaged with AFM they were required to be securely attached to the substrate or the cell would be dislodged/removed by movement of the AFM tip. The etched glass cover slips provided a reference that enabled return to the locations of interest after the sample was moved to the stage of the AFM.

Cells were imaged with AFM in tapping mode (Hansma et al., 1994) using a Digital Instruments Dimension 3100 AFM. The fluid cell (Digital Instruments, #DTFML) was fitted with a silicon nitride tip (Digital Instruments, #DNP-20). The V-shaped cantilever was 200 μm in length, yielding a nominal spring constant of 0.32 N/m. The tip was square pyramidal in shape with a nominal tip radius of curvature of 20–60 nm. The laser was aligned on to the top of the cantilever and adjustments of alignment were made to the photo detector for maximum sensitivity. Course approach to the surface was performed until the fluid cell entered the culture medium. At that time, the alignment was adjusted and the resonance frequency determined (6–8 kHz) for maximum tip oscillation. A drive amplitude of 400–600 mV was applied to obtain a free amplitude of 0.5 V RMS. This was performed at 200 nm from the sample surface. The tip was then brought into “contact” with the surface. Control parameters were optimized to minimize the force on the sample. The set point parameter was increased until the tip lifted off the sample surface. The set point was then decreased by the smallest increment allowing for minimal force on the sample. Other parameters such as scan size, angle, rate, and proportional and integral gains were adjusted to optimize the image. The image fields (≈10 μm<sup>2</sup>) were obtained at 0.4–0.6 Hz; thus 2–10 min were required to complete a raster scan of the entire sample. Small area images comprising neurites or growth cones usually required 2 min to complete prior to the next period of imaging, while large cells could take 5–10 min to complete. It is important to note that some features of the anatomy that may

change within this time constant would not be a portion of the composite image.

Both height and amplitude data were used to image the surface topography. AFM height scans provide surface topography data with unparalleled resolution. Lateral resolutions of 1 nm and vertical resolutions of 0.1 nm are possible when operating in contact mode in air or vacuum. AFM operation in tapping mode and in fluids, as performed in this investigation, slightly reduces this resolution but also minimizes damage to the soft biological material. Amplitude data are more sensitive to changes in height. This provided increased information concerning the surface topography but not accurate height information. Fig. 1 shows a height image of a living sympathetic neuron analyzed for quantitative profiles of features of interest, and reveals how any portion of a complete image can be quantitatively measured. Panel A provides the original height data of the growth cone with the corresponding color bar for z-axis values. Index lines have been drawn on the image to delineate areas of interest. The profiles along each colored index line are provided in panel B. The differences in height and width of the neurite, growth cone, and microspikes are apparent. Panel C provides a 3-D representation of the height data using the Digital Instruments system software. Panel D is an optical micrograph of the cultured cells prior to imaging with the AFM.

### 2.4. Image comparison

The dramatically different image collection modes of scanning confocal microscopy and AFM make any image comparison a difficult task. However, it is useful to compare images using a common format. The AFM instrument operating in the tapping mode measures topography by tapping the surface with an oscillating probe tip, so that the tip makes contact with the sample only for a short duration in each oscillation cycle. In contrast to atomic force microscopy, confocal microscopy is a method based on traditional far-field optics. Detectors in CLSM collect photons emitted by the fluorescent labels introduced into a biological sample. The instrument utilizes an optical pathway typical of conventional optical microscopes. The presence of a confocal aperture, stopping the fluorescence signal from out-of-focus optical planes, makes this technique capable of collecting 3-D images. It is very important to recognize that the concept of 3-D imaging in confocal systems differs significantly from what is taken to be 3-D visualization using AFM methodology. Only a confocal instrument collecting backscattered light (BSL) from a non-transparent object might be considered as a far-field optics counterpart to AFM. Such BSL images are limited to the surface of the observed sample, while the internal structure would remain unknown. However, CLSM using fluorescence mode can collect emission originating in the interior of a biological sample. This means that a confocal microscope can record a 3-D array of numbers representing intensity of fluorescence from all the scanned voxels within the analyzed volume of the sample. Such a data structure poses a number

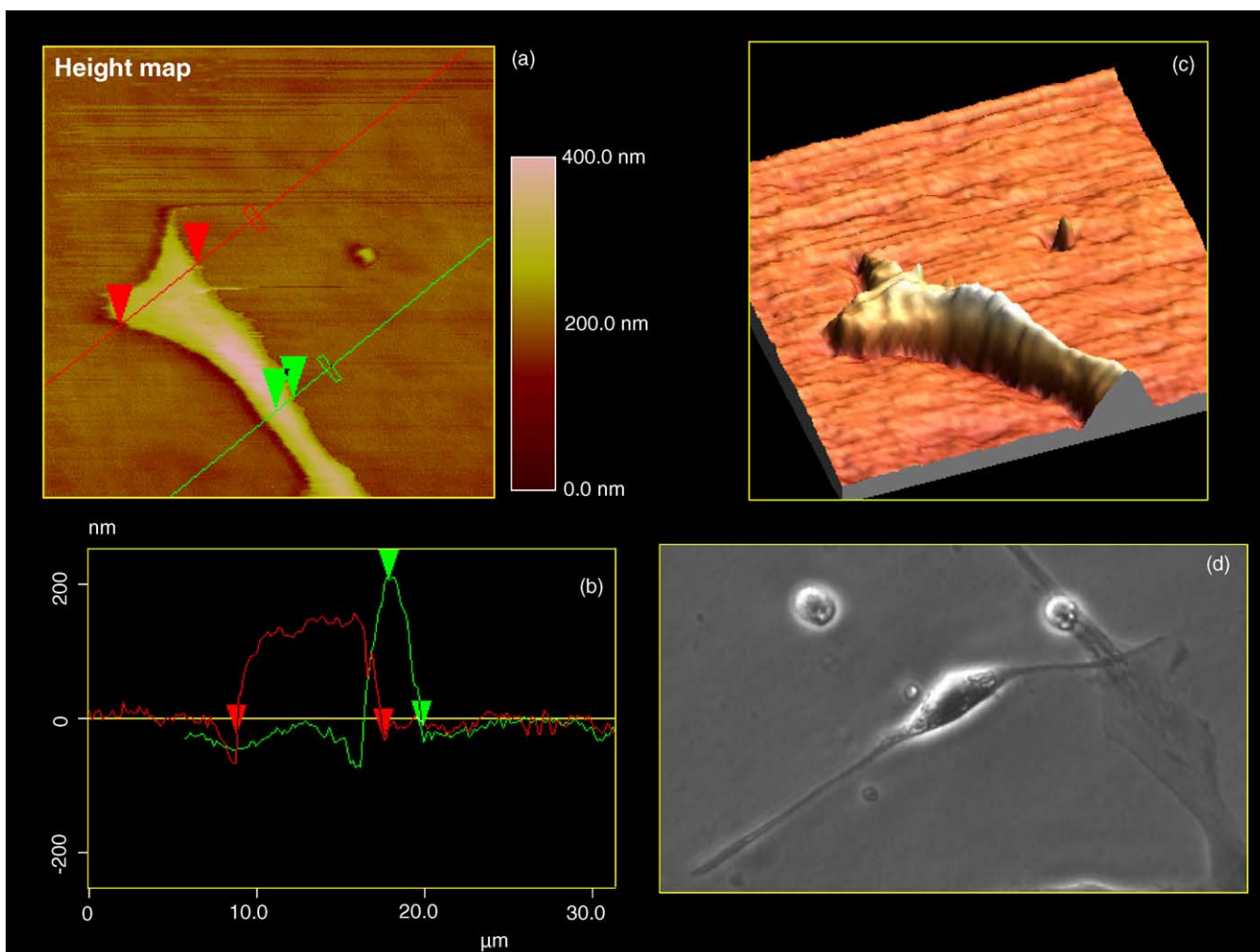


Fig. 1. AFM Imaging and quantification of structure. The ‘height mode’ image of a sympathetic neuron growth cone is shown in panel (a). The color table provides height information in the Z-axis. Note the two index lines crossing the growth cone (red and green). The height profiles along these lines are provided in the graph below (panel b). In Panel (c) the height data have been manipulated for a 3-D view of the growth cone. The micrograph in panel (d) shows cultured cells typical of those used in these studies.

of problems for visualization and display. In their simplest form, confocal data can be shown as a series of individual sections. However, more often the data are presented using volumetric display techniques, like ray-tracing. The structure of AFM data is simpler: an image is represented by a 2-D array of numbers, in which the values correspond to deflections of the AFM cantilever caused by the probe-sample interactions. Visualization of AFM data is usually attained by creation of a simple surface display (elevation map). Even though this visualization technique gives the impression of three-dimensionality, it is not fully 3-D. Nevertheless, it is both instructive and convenient to refer to the AFM images presented in this paper as 3-D.

The limits of resolution characteristic of AFM and CLSM are also very different. The resolution of far-field light microscopes is restricted by the diffraction limits of the microscope objective. AFM instruments can resolve sub-nanometer structures because the resolution is governed by different principles and is limited by the smallest resolvable

vertical displacement of the tip. CSLM images are inherently noisy as a result of the statistical fluctuations associated with photon detection (Young, 1996). The imaging noise characteristic of the confocal instrument is not independent of the signal, is not Gaussian, and is not additive (Young, 1996). The noise inherent in AFM imaging is related to the fact that the AFM tip undergoes thermal motion; therefore, its excursion increases with temperature. Lastly,  $z$ -resolution of CLSM for any given wavelength is always approximately twice as inaccurate as its resolution in the  $x/y$  plane. Therefore, height values calculated from 3-D images acquired by CLSM are less precise than  $x/y$  measurements obtained from the same datasets. In contrast, the AFM instrument’s  $z$ -axis resolution is associated with the actual vertical excursion of the tip. These movements can be extremely small—sometimes less than a fraction of a nanometer—producing datasets rich in precise  $z$ -axis detail. All of the aforementioned differences between CLSM and AFM image formation contribute to the interpretation of the images.

In order to find a common ground for an AFM–CLSM image comparison we represented both AFM and CLSM datasets as elevation maps with color-coded height. Although the effective  $xy$ -resolutions of AFM and confocal images in our experimental set up were similar, the  $z$ -resolution of CLSM was always dramatically inferior. The AFM and CLSM data files were visualized using Image J, Volume J and Surface J packages (Abramoff and Viergever, 2002). Since AFM images represent topography of cells, the contrast is high and the structures are well defined. The contrast in CLSM images arises from fluorescence staining with FM 1-43 dye. This stain is readily internalized by living neurons. However, distribution of the dye within the plasma membrane and lipid vesicles inside cells is not uniform. Therefore, it must be emphasized that the visualization of CLSM data shows the localization of FM 1-43, through which the topology of the cell is defined. The dimensions of the features shown on the collected images demonstrate very high levels of similarity considering all the listed differences in the imaging modalities used.

### 3. Results images (confocal and AFM)

#### 3.1. Soma

The neuron cell body as imaged by AFM was typically 10–20  $\mu\text{m}$  in diameter and 1–4  $\mu\text{m}$  in height consisting of folds, ridges, and spines projecting vertically from the soma surface up to 1  $\mu\text{m}$ . This is quite different from the common perception of a neuronal cell body as that of a relatively smooth, dome-shaped structure surrounded by dynamic flattened lamellipodium and a ruffled membrane (Leviton and Kaczmarek, 1991). A flattened lamellipodium was also seen by AFM but again with spiny projections and steep ridges projecting up to 200 nm from this region. Previous researchers have detected axonal spines (Peters et al., 1991) on fixed cell bodies or predicted spines in living cells but never captured them as dynamic entities varying with time. These complex shapes were not characteristic of an individual cell under scrutiny as they constantly shift from one form to another over a period of minutes. Therefore, the 3-D cytoarchitecture of

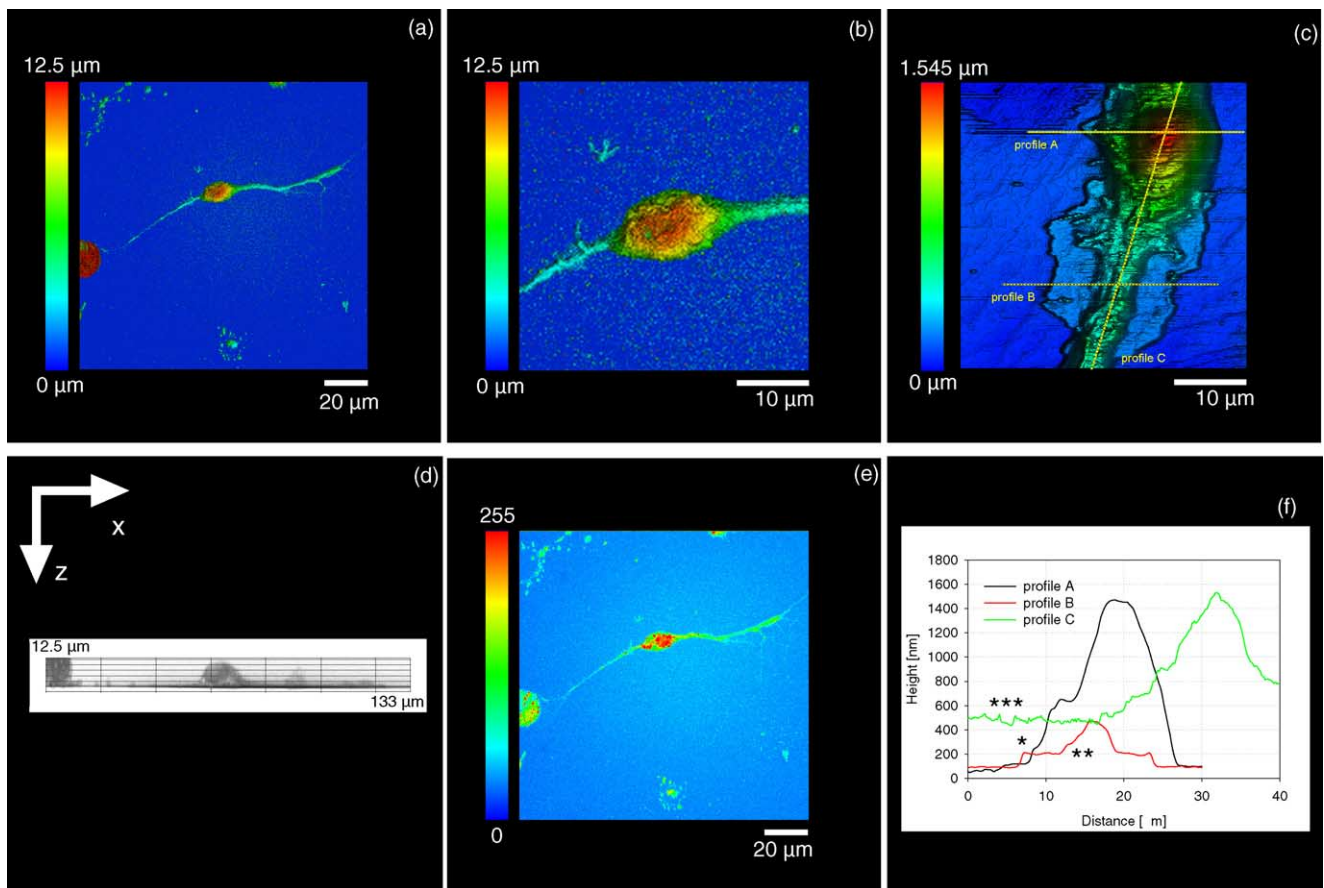


Fig. 2. Comparison of confocal and AFM data obtained from study of a neuron cell body. Image (a) is a CLSM height map of a typical DRG cell body and extending neurites. Image (b) is an electronic magnification of (a) focusing on the cell body. The pixel size of this image is identical to that obtained by the AFM image shown in (c). Image (d) presents the orthogonal view of the confocal dataset shown in (a), while image (e) shows the concentration map of FM 1-43 dye; (c) is a typical AFM image including a color scale providing height information. The dotted lines drawn on this image represent profiles shown in (f). Profile B gives fine detail of the incremental steps from the substrate to the lamellipodium (\*) and the transition to the cell neurite (\*\*). Profile C reveals ridges and spikes extending up to 100 nm above the surface of the living neurite (\*\*\*)

microfilaments and microtubules subtending these complex shapes are in dynamic stages of assembly and disassembly on a minute-by-minute basis. Fig. 2 provides images acquired using CLSM and AFM on DRG cell bodies. For various technical and logistical reasons, we were not able to image the same living cell with both instruments. Image 2a is a confocal height-map of a typical DRG cell body and extending neurites. Image 2b is an electronic magnification of image 2a focusing on the cell body. The pixel size of this image is identical to that obtained by the AFM shown in Fig. 2c. Image 2d presents the orthogonal view of the confocal dataset shown in Fig. 2a, and image 2e shows the concentration map of FM 1-43 dye. Fig. 2c is a typical AFM image of a DRG cell body. As with the confocal images, the color scale provides height information. The dotted lines drawn on this image represent the profile lines shown in Fig. 2f. Profile A revealed a cell body of 18  $\mu\text{m}$  diameter and 1.4  $\mu\text{m}$  high. Profile B shows the clear steps from the substrate to the lamellipodium (\*) and the transition to the cell neurite (\*\*). Profile C revealed ridges and spikes extending up to 100 nm above the surface of the

living neurite (\*\*). These ridges and spikes were dynamic structures, appearing and disappearing during the period of time required for the AFM image collection. Both confocal and AFM images revealed similar shapes and overall architectures of the soma. However, it should be remembered that the comparatively low  $z$ -resolution of a far-field confocal system does not permit accurate evaluation of the height, thus explaining the discrepancy between height data of the AFM and confocal systems. The resolution capabilities of the AFM, particularly in the  $z$ -axis, provide extremely accurate measurements of the cell body size and shape and revealed the dynamic vertical extensions.

### 3.2. Growth cone

Levitan and Kaczmarek (1991) have also described the growing tip of a neural cell process as a central flattened core with extending filopodium and connecting lamellipodium continuously changing its 2-D form. However, AFM also revealed relatively tall ridges and spine-like projections in

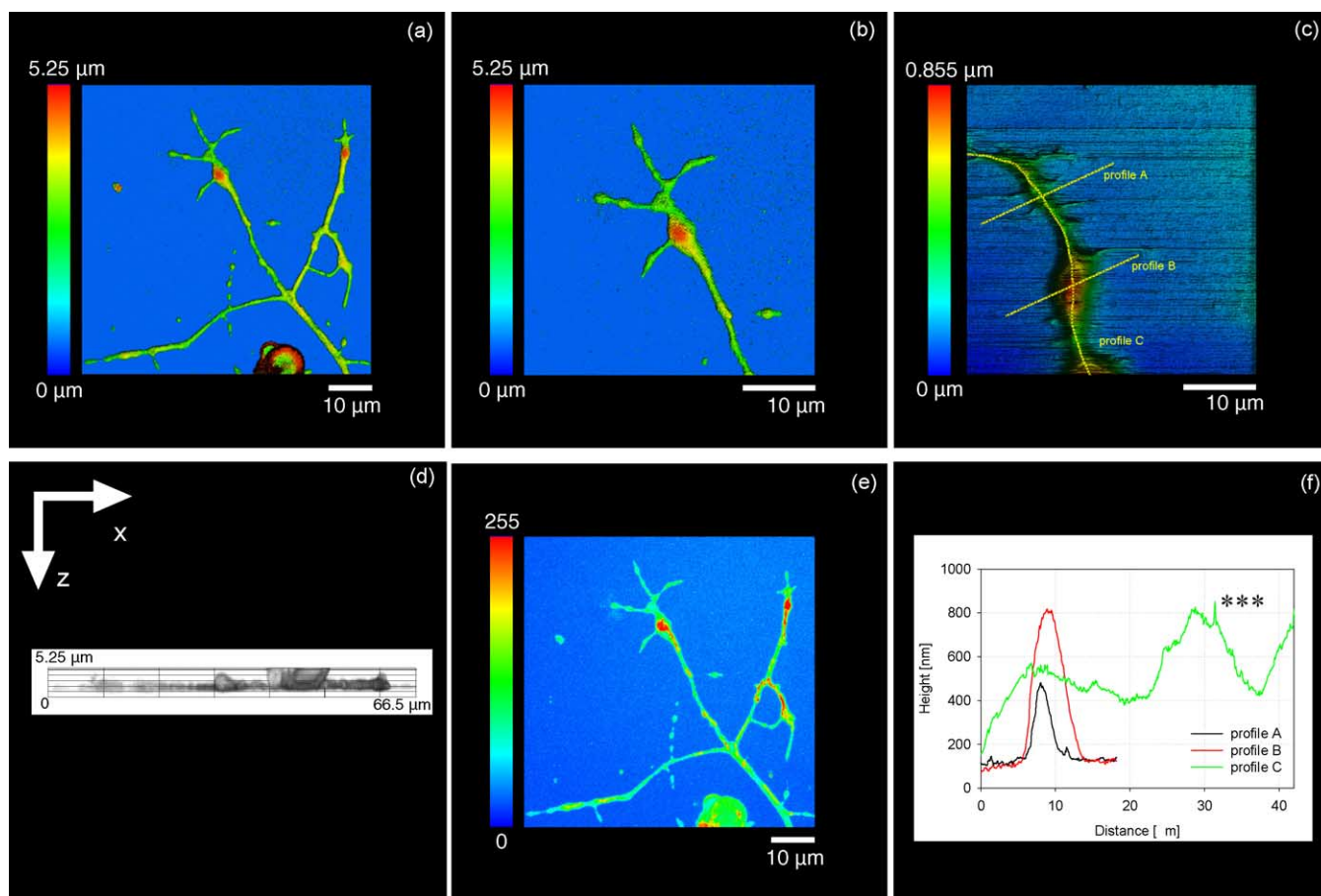


Fig. 3. Growth cone comparison of confocal and AFM data obtained from study of a growth cone: (a) is a CLSM height map of a typical DRG neurite; (b) is an electronic magnification, focusing in on the growth cone. Image (d) demonstrates the orthogonal view of the confocal dataset shown on (a), while image (e) shows the FM 1-43 concentration map; (c) is a typical AFM height image of a DRG growth cone with its associated color bar. The dotted lines in this image are shown as profiles in (f). Profile (c) reveals a backbone-like structure extending from the neurite terminus into the growth cone region. Spikes extending up to 70 nm above the surface of the neurite and growth cone regions (\*\*\*) were again dynamic in nature, changing from one image to another. Microspikes are also seen in panel (c) extending horizontally from the growth cone.

the vertical axis of growth cones. Likewise, these ‘thorns and protuberances’ were continuously changing and often associated with a ridge-like ‘backbone’ extending into the growth cone proper. The terminal ends of neurites measured by AFM averaged  $6.45 \pm 2.4 \mu\text{m}$  wide and  $387.5 \pm 193.1 \text{ nm}$  high ( $n=25$ ). The vertical ridges and spines observed near the end of the neurite averaged  $93.27 \pm 71.9 \text{ nm}$  in height. The area of growth cones averaged  $10.5 \pm 2.94 \mu\text{m}$  wide and  $259.5 \pm 182 \text{ nm}$  high with vertical projections averaging  $248.3 \pm 148.9 \text{ nm}$  ( $n=25$ ). In addition, AFM resolved fine hair-like structures projecting horizontally from the lateral walls of the nerve fibers. Individual ‘hairs’ ranged in caliber from  $100 \text{ nm}$  to  $1 \mu\text{m}$  and  $1\text{--}2 \mu\text{m}$  in length. Like the relatively massive ridges and spines, these minute structures also extended and retracted between scans—changing shape, or disappearing all together. Finally, we did not see any evidence of an equilibrium stage of cell architecture where all—or even most—of these topographical features remained static. Fig. 3 provides images of a DRG growth cone acquired with both CLSM and AFM. Fig. 3a is a CLSM height map of a typical DRG. Fig. 3b shows an electronic magnification of the growth cone. Image 3d demonstrates the orthogonal view of the confocal dataset shown in Fig. 3a, while image 3e shows the FM 1-43 concentration map. Fig. 3c is a typical AFM height-image of a DRG growth cone, and Fig. 3f shows the profiles along the dotted index lines. Profile A provides measurements of the growth cone:  $3 \mu\text{m}$  wide and  $388.5 \text{ nm}$  high. Profile B shows this neurite to be  $8 \mu\text{m}$  wide and  $669.3 \text{ nm}$  high. Profile C reveals a backbone-like structure extending from the neurite terminus into the growth cone region. Spikes extending up to  $70 \text{ nm}$  above the surface of the neurite and growth cone regions (\*\*\*) were again dynamic in nature, shifting in form from one acquired image to the next. Microspikes were also present on the neurite shown in panel 2c, extending horizontally from the growth cone. These projections ranged from  $40 \text{ nm}$  to  $2 \mu\text{m}$  wide and  $100\text{--}200 \text{ nm}$  high. These projections were also dynamic, appearing and disappearing between periods of image acquisition. Both the confocal and AFM images reveal similar shapes and overall architectures of the growth cones. Again, the low  $z$ -resolution of a far-field confocal system did not permit an accurate evaluation of the height. Moreover, AFM was capable of recording the continuously changing height of growth cones and their projections.

#### 4. Discussion

This is the second report in a series in which AFM technology has been used to evaluate the 3-D architecture of living neurons. In this report, the AFM data have been compared to CLSM images and evaluated after both datasets were visualized with the same technique and tools. The AFM has revealed unexpected soma architectures, confirmed by live-cell CLSM observation. AFM has also revealed dynamic vertical projections from the growth cone and surrounding

lamellipodium as well as fine structures projecting horizontally. These features are similar to those captured by scanning electron microscopy, but instead on living cells.

A biological role for the rapidly forming and transitory vertical projections is currently unknown. While filopodia have sensory and motor capabilities which combine to guide the growing process to a suitable location for connection, the extensions are nominally thought to be in the plane of growth. While this may be typical for cultured cells on a flat substrate, in vivo one can imagine cytoplasmic extensions would develop in all three dimensions. The fine hair-like structures extending in the plane of growth may actually be axonal spines, although these are generally reported to be much larger in size. The resolution of AFM has allowed us to capture and characterize these vertical and horizontal extensions with much greater detail (see also McNally and Borgens, 2004). The versatility of the AFM will also allow us to investigate the form and function of these projections, providing further explanation for their appearance and/or retraction. Additionally, the AFM will be employed by our laboratory to study physical properties of the membrane, sub-cellular components, and the responses to stimuli, such as endotoxins, mechanical injury, and the repair process.

#### Acknowledgements

We thank Professor Richard Borgens, Director, Center for Paralysis Research (CPR) for many useful discussions and guidance. We gratefully acknowledge the technical assistance of Ms. Judy Grimmer, cell culture lab, CPR. We also thank Professor Michael Melloch, School of Electrical and Computer Engineering, for the use of the AFM. This work was supported by general funds from the CPR, a generous gift from Mrs. Mari Hulman George, and support of the joint Purdue University/Indiana University program in Central Nervous System Injury by the State of Indiana (HB1244).

#### References

- Abramoff MD, Viergever MA. Computation and visualization of 3-D soft tissue motion in the orbit. *IEEE Trans Med Imaging* 2002;21:296–304.
- Binnig G, Quate CF. Atomic force microscopy. *Phys Rev Lett* 1986; 56:930–3.
- Gallant PE, Galbraith JA. Axonal structure and function after axolemmal leakage in the squid giant axon. *J Neurotrauma* 1997;14:811–22.
- Hansma PK, Cleveland JP, Radmacher M, Walters DA, Hillner PE, Bezanna M, et al. Tapping mode atomic force microscopy in fluids. *Appl Phys Lett* 1994;64:1738–40.
- Henderson E, Sakaguchi DS. Imaging F-actin in fixed glial cells with a combined optical fluorescence/atomic force microscope. *Neuroimage* 1993;1:145–50.
- Hennig AK, Cotanche DA. Regeneration of cochlear efferent nerve terminals after gentamycin damage. *J Neurosci* 1998;18:3282–96.
- Higgins D, Banker G. Primary dissociated cell cultures. In: *Culturing Nerve Cells*. Cambridge, MA: MIT Press; 1998.

- Jena BP. Atomic force microscope: providing new insights on the structure and function of living cells. *Cell Biol Int* 1997;21:683–4.
- Lal R, Drake B, Blumberg D, Saner DR, Hansma PK, Feinstein SC. Imaging real-time neurite outgrowth and cytoskeletal reorganization with an atomic force microscope. *Am J Physiol* 1995;269:275–85.
- Levitan IB, Kaczmarek LK. *The Neuron Cell and Molecular Biology*. New York: Oxford University Press, New York; 1991.
- Mahanthappa NK, Patterson PH. Culturing mammalian sympathetic adrenal derivatives. In: *Culturing Nerve Cells*. Cambridge, MA: The MIT Press; 1998.
- Matsumoto B. *Cell Biological Applications of Confocal Microscopy*. San Diego: Academic Press; 2002.
- McNally H, Borgens R. Three-Dimensional imaging of living and dying neurons with atomic force microscopy. *J Neurocytol* 2004;33:251–8.
- Melling M, Hochmeister S, Blumer R, Schilcher K, Mostler S, Behnam M, et al. Atomic force microscopy imaging of the human trigeminal ganglion. *Neuroimage* 2001;14:1348–52.
- Morris VJ, Kirby AR, Gunning AP. *Atomic Force Microscopy for Biologist*. London: Imperial College Press; 2001.
- Niell CM, Smith SJ. Live optical imaging of nervous system development. *Annu Rev Physiol* 2004;66:771–98.
- Parpura V, Haydon PG, Henderson E. 3-D imaging of living neurons and glia with the atomic force microscope. *J Cell Sci* 1993;104(Pt 2):427–32.
- Pawley J. *Handbook of Biological Confocal Microscopy*. New York: Plenum Press; 1995.
- Peters A, Palay SL, Webster HF. *The Fine Structure of the Nervous System*. New York: Oxford University Press, New York; 1991.
- Piston DW. Choosing objective lenses: the importance of numerical aperture and magnification in digital optical microscopy. *Biol Bull* 1998;195:1–4.
- Ricci D, Grattarola M, Tedesco M. Growth cones of living neurons probed by atomic force microscopy, methods in molecular biology. In: *Atomic Force Microscopy Biomedical Methods and Applications*. Totowa, New Jersey: Humana Press; 2004.
- Ryan TA. Presynaptic imaging techniques. *Curr Opin Neurobiol* 2001;11:544–9.
- Ryan TA, Reuter H, Smith SJ. Optical detection of a quantal presynaptic membrane turnover. *Nature* 1997;388:478–82.
- Sah R, Schwartz-Bloom RD. Optical imaging reveals elevated intracellular chloride in hippocampal pyramidal neurons after oxidative stress. *J Neurosci* 1999;19:9209–17.
- Schabert F, Knapp H, Karrasch S, Haring R, Engel A. Confocal scanning laser—scanning probe hybrid microscope for biological applications. *Ultramicroscopy* 1994;53:147–57.
- Tojima T, Yamane Y, Takagi H, Takeshita T, Sugiyama T, Haga H, et al. 3-D characterization of interior structures of exocytotic apertures of nerve cells using atomic force microscopy. *Neuroscience* 2000;101:471–81.
- Vesenska J, Mosher C, Schaus S, Ambrosio L, Henderson E. Combining optical and atomic force microscopy for life sciences research. *Biotechniques* 1995;19:240–48, p. 849, 852–243.
- Weissmuller G, Garcia-Abreu J, Mascarello Bisch P, Moura Neto V, Cavalcante LA. Glial cells with differential neurite growth-modulating properties probed by atomic force microscopy. *Neurosci Res* 2000;38:217–20.
- Young I. Quantitative microscopy. *IEEE Eng Med Biol* 1996;15:59–66.